

Article

## Microfluidic Devices for Blood Fractionation

Han Wei Hou <sup>1,2</sup>, Ali Asgar S. Bhagat <sup>1</sup>, Wong Cheng Lee <sup>1,3</sup>, Sha Huang <sup>4</sup>, Jongyoon Han <sup>1,4,5</sup>  
and Chwee Teck Lim <sup>1,2,3,6,7,\*</sup>

<sup>1</sup> BioSystems and Micromechanics (BioSyM) IRG, Singapore-MIT Alliance for Research and Technology (SMART) Centre, Singapore 117543; E-Mails: hwhou@nus.edu.sg (H.W.H.); ali.bhagat@gmail.com (A.A.S.B.); wlee@nus.edu.sg (W.C.L.)

<sup>2</sup> Division of Bioengineering, National University of Singapore, Singapore 117576

<sup>3</sup> NUS Graduate School for Integrative Sciences and Engineering, National University of Singapore, Singapore 117456

<sup>4</sup> Department of Electrical Engineering & Computer Science, Massachusetts Institute of Technology, Cambridge, MA 02139, USA; E-Mails: huangsha@mit.edu (S.H.); jyhan@mit.edu (J.H.)

<sup>5</sup> Department of Biological Engineering, Massachusetts Institute of Technology, Cambridge, MA 02139, USA

<sup>6</sup> Department of Mechanical Engineering, National University of Singapore, Singapore 117576

<sup>7</sup> Mechanobiology Institute, Singapore 117411

\* Author to whom correspondence should be addressed; E-Mail: ctim@nus.edu.sg; Tel.: +65-6516-6564; Fax: +65-6772-2205.

Received: 11 May 2011; in revised form: 27 June 2011 / Accepted: 6 July 2011 /

Published: 20 July 2011

---

**Abstract:** Blood, a complex biological fluid, comprises 45% cellular components suspended in protein rich plasma. These different hematologic components perform distinct functions *in vivo* and thus the ability to efficiently fractionate blood into its individual components has innumerable applications in both clinical diagnosis and biological research. Yet, processing blood is not trivial. In the past decade, a flurry of new microfluidic based technologies has emerged to address this compelling problem. Microfluidics is an attractive solution for this application leveraging its numerous advantages to process clinical blood samples. This paper reviews the various microfluidic approaches realized to successfully fractionate one or more blood components. Techniques to separate plasma from hematologic cellular components as well as isolating blood cells of interest including certain rare cells are discussed. Comparisons based on common separation metrics including efficiency (sensitivity), purity (selectivity), and

throughput will be presented. Finally, we will provide insights into the challenges associated with blood-based separation systems towards realizing true point-of-care (POC) devices and provide future perspectives.

**Keywords:** blood separation; microfluidics; cell separation; enrichment; disease detection and diagnosis

---

## 1. Introduction

Blood, perhaps the most important biological fluid, performs many fundamental functions to maintain homeostasis; from transporting nutrients and oxygen to tissues and organs to regulating pH and temperature. It also provides an efficient transit system through the vascular network for transport of immune cells for defense against foreign microbes and wound healing. As blood contains a myriad of information about the functioning of the human body, complete blood analysis has been a primary diagnostic test in our healthcare system. Broadly, plasma and cells constitute the two main blood components each with ~60% and 40% volume fractions respectively. The blood cellular components mainly consist of red blood cells (RBCs), leukocytes and platelets. Other rare-cells including fetal cells during pregnancy and epithelial tumor cells in cancer patients may also be found circulating in blood. Of the ~5 billion cells per milliliter of blood, red blood cells (RBCs) make up >99% of all cellular components. Due to the vast majority of RBCs, fractionating the various target components from blood has been a challenging problem both from a medical and engineering perspective.

Conventional plasma and leukocyte separation methods have relied on membrane-based filtration. However, the high cellular fractions lead to membrane clogging and compromise separation efficiency. To address this, enormous progress has been made in the past few years in the area of microfluidics based blood component separations. Microfluidics is the science of studying fluid flow behavior at the microscale and the development of miniaturized analysis systems that take advantage of the unique physics emergent at these small scales [1,2]. Microfluidics leverages its many distinct advantages such as low sample volume for processing blood, as these samples are precious and rare especially in the case of neonatal care. A comprehensive review of processing blood on a microchip discussing the various sample preparation challenges, cell separation methods and integrated blood analysis modules was presented by Toner and Irimia [3]. However, the field of microfluidics based blood fractionation has significantly advanced since then and a review of the various microfluidic approaches developed in the past few years is warranted.

In this paper we review recent microfluidic methods realized to successfully fractionate one or more blood components. Although microfluidic based cell separation techniques have been extensively reviewed in the past, to our knowledge this is the first attempt to summarize microfluidics based techniques to separate the individual blood components [4-9]. Detailed description of the various separation principles for each component will be discussed and comparisons based on separation metrics including efficiency (sensitivity), purity (selectivity), and throughput will be drawn. The readers are encouraged to read the original papers for additional details. Analysis of these individual components for clinical diagnosis or fundamental studies is beyond the scope of this review.

## 2. Plasma Separation

Many clinical tests and research assays frequently require the removal of blood cells from plasma for downstream analysis and diagnosis. A simple diagnostic test of blood plasma for biological substances such as cholesterol, glucose and lactate can be used to evaluate the general state of health of various internal organs. The quantification of individual plasma proteins is also routine and important for diagnosis and monitoring of many diseases including paraproteinaemias, hemoglobinopathies, and genetic abnormalities [10,11]. However, it is critical to remove the large volume of interfering blood cells from whole blood so that the purified plasma can be assessed and diagnosed accurately.

Traditionally, plasma is extracted from blood in laboratories and clinics by centrifugation with conventional bench-top centrifuges which are known to be expensive, time consuming and labor intensive. The practice of centrifugation has also been realized on the microscale using compact disk-like platforms with manifolds and a spinning motor plate to achieve centrifugal pumping, fostered by the need to develop an integrated total analysis system [12,13]. Haeberle and coworkers designed a decanting structure on a rotating disk for the extraction of plasma [12]. The technique efficiently extracts 2  $\mu\text{L}$  plasma from a 5  $\mu\text{L}$  blood sample rotated at 40 Hz frequency within 20 s. The extracted plasma contained  $<0.11\%$  blood cell concentration independent of rotation frequency. Recently, an innovative method to isolate plasma for resource limited settings has been demonstrated by Wong *et al.* using an egg beater as a hand-powered centrifuge [Figure 1(A)] [14]. By spinning the paddle, human whole blood loaded into polyethylene (PE) tubing attached to the end of the paddle of the egg beater is centrifuged. The blood cells settle down at the distal end of the PE tubing while plasma extracted from the supernatant can be used to perform diagnostic assays. The technique extracts  $\sim 58 \mu\text{L}$  plasma from 100  $\mu\text{L}$  whole blood after 8 min of centrifugation with very high purity (cell concentration  $\sim 5 \times 10^4 \text{ mL}^{-1}$ ). However, during centrifugation the sedimented blood cells can easily lyse (RBCs hemolysis), thereby releasing intracellular components which contaminate the plasma sample [14]. To overcome this limitation, several microfluidic techniques for plasma isolation from blood have been recently reported.

Perhaps the most common way of separating plasma from blood cells using microfluidic devices is based on the principle of particle retention. These devices frequently involve the use of micromachined filters or meshes to retard or block blood cell movement, thereby allowing the collection of the plasma portion of blood. In particular, comb and weir-type filter structures with well defined geometries have been designed and demonstrated [15-17]. Designing weirs with a gap size of 0.5  $\mu\text{m}$ , VanDelinder and Groisman reported a cross-flow based microfluidic device for continuous plasma separation [16]. The 0.5  $\mu\text{m}$  gap permits the flow of plasma while impeding the RBCs, leukocytes and platelets. The device is capable of operating continuously for an hour extracting  $\sim 8\%$  plasma at 0.65  $\mu\text{L}/\text{min}$  throughput and  $<0.1\%$  hemolysis. Similar design employing 0.5  $\mu\text{m}$  gap transverse-flow microfilters was also reported by Crowley and Pizziconi [17]. Size-exclusion based techniques relying on integrated microporous fleece or membranes have also been developed [18,19]. Moorthy and Beebe fabricated porous filters inside a microchannel using emulsion photo-polymerization with the porosity of the filter being a function of the pre-polymer mixture constituting 2-hydroxyethyl methacrylate (HEMA, monomer), ethylene glycol dimethacrylate (EGDMA, cross-linker), and 2,2-dimethoxy-2-phenyl-acetophenone (DMPA, photo-initiator) in water. The device was tested with diluted blood (1:20) to demonstrate

separation. However, both the weir-based and membrane-based devices frequently suffer from RBCs contamination due to their extremely high deformability. This also poses enormous challenge to the fabrication as very small pore size or filters on the order of 1  $\mu\text{m}$  or less are required to retain the RBCs effectively. Moreover, as the geometrical features of these devices become smaller, clogging becomes a major concern and blood has to be diluted before separation thereby compromising throughput and operation time. Another novel method to separate plasma from whole blood using bead-packed microchannels acting as filters has been demonstrated recently [Figure 1(B)] [20]. Blood introduced into the channel is driven by the capillary force induced by the bead column. As the RBCs movement is impeded by the packed beads, cell-free plasma is driven through the bead column. Without the use of microfilters, this technique minimizes RBCs clogging, but is unsuitable for rapid clinical diagnostics due to long separation time as a result of slow capillary action.

In order to circumvent the aforementioned problems, several groups have investigated RBC depletion using flow through devices which function solely on inherent hydrodynamic separation mechanisms. Separating blood plasma based on the inherent hydrodynamic separation mechanisms frequently rely on the Zweifach-Fung effect, also known as bifurcation law [21-23]. The technique exploits the tendency of cells at branching points of microchannels to flow into the wider channel having a higher flow rate. By varying the channel widths of the daughter channels, Yang *et al.* reported a minimum flow rate ratio of 6:1 required between the main and smaller branching channels to obtain successful blood plasma separation [Figure 1(C)] [21]. The plasma selectivity obtained was close to 100% and was independent of the inlet hematocrit levels while the collected plasma volume varied from 15 to 25% depending on the inlet hematocrit levels. Plasma separation from blood cells has also been achieved using “plasma skimming” or the Fahraeus effect. In microchannels flow under Poiseuille conditions, the highly deformable RBCs migrate towards the axial centre of the microchannels parallel to flow. This creates a lower cell concentration or “cell free” region near the channel walls where plasma can be extracted easily. Jaggi *et al.* demonstrated the use of a high-aspect ratio microchannel device with many vertical channel bifurcations arranged in parallel to extract plasma from blood [24]. The device permits very high throughput operating at relatively high flow rates of between 2 to 5 mL/min with high separation (cell depletion) efficiency ( $\sim 90\%$ ) at 4.5% hematocrit. However, the cell depletion efficiency drops significantly to  $\sim 30\%$  when tested with physiological hematocrit (45%). Blatter *et al.* combined centrifugal forces with plasma skimming to demonstrate plasma extraction using a simple microchannel bend [25,26]. The centrifugal forces results in differing settling velocities between the cells and plasma resulting in the collection of cell free plasma near the inner wall of the microchannel following the bend region. As this technique also relies on plasma skimming, blood dilution is necessary as a  $\sim 90\%$  cell depletion efficiency at  $\sim 5\%$  hematocrit reduces to  $\sim 40\%$  at 45% hematocrit.

**Figure 1.** Plasma separation from blood. **(A) left:** Schematic diagram shows the centrifugation based separation principle using an egg beater with the blood-filled PE tubing attached to the paddle (inset illustrates the photograph of a manual hand-powered egg beater). *centre:* Phase contrast images showing RBCs concentrations in the plasma layer and cell pellet region of the PE tubing after 10 min spinning. *right:* Graph showing the plasma volume generated against centrifugation time from a 100  $\mu$ L blood sample. Reprinted with permission from [14] copyright 2008, The Royal Society of Chemistry; **(B) left:** Graphical illustration of plasma separation from whole blood using icrobeads-packed microchannel. As blood flows through the hydrophilic channel by capillary forces, RBCs movement is impeded by the packed beads while the plasma (yellow) continues to move forward. *right:* Photograph showing the formation of four separated regions as blood flows through the bead-packed channel corresponding to different stages of plasma separation. Figure reproduced from [20], copyright 2010, with kind permission from Springer Science + Business Media, LLC; **(C) Plasma separation using hydrodynamics effects. left:** Schematic representation of the Zweifach–Fung effect in which RBCs travel into the daughter channel with higher flow rate when the flow rate ratio is more than 2.5 times compared to the smaller daughter channel. The image at the bottom shows the schematic of the actual plasma separation device with the plasma separation region consisting of 5 bifurcated plasma skimming channels. *centre:* Photograph of the blood plasma separation region at a flow rate of 10  $\mu$ L/h. *right:* Comparison between experimental and computational fluid dynamics (CFD) simulation results of the total plasma separation volume percent with respect to the upstream microchannel hematocrit level. The numbers indicate at each data point represent the inlet hematocrit levels. Redrawn with permission from [21], copyright 2006, The Royal Society of Chemistry.

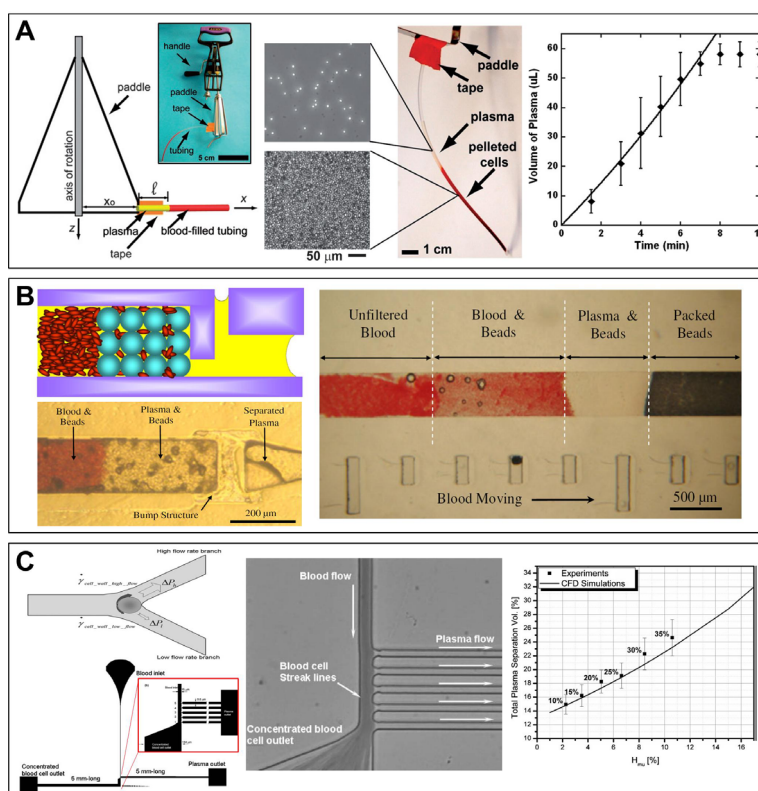
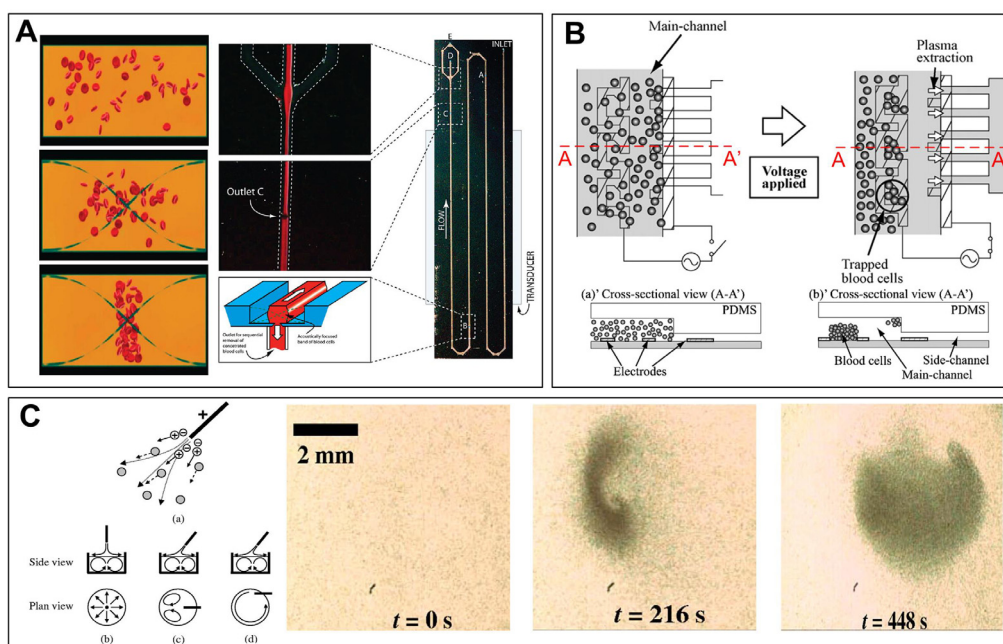


**Figure 2.** (A) Plasma separation using acoustophoresis. Cross-sectional schematics of a microchannel excited by a  $\lambda/2$  wavelength ultrasonic standing wave indicating the focusing of the RBCs at the channel center by the primary acoustic radiation force. By designing a multiple outlet system enriched blood cell fractions are removed from the center of the channel while clean plasma fraction can be withdrawn from the side. A transducer placed underneath the chip generates an ultrasonic standing wave between the channel walls perpendicular to the flow. Reprinted with permission from [27], copyright 2009, American Chemical Society; (B) Plasma separation using dielectrophoresis (DEP). The image shows the top and cross sectional views of plasma extraction principle from diluted blood (1:9) in the presence of electric field gradient. The strong DEP forces traps ~97% of RBCs at the electrodes extracting ~300 nL of plasma from 5  $\mu$ L of blood. Figure reprinted from [33], copyright 2010, with permission from Elsevier; (C) *left* Schematic illustrating the principle of inducing swirling flows in microchambers by bulk electrohydrodynamics thrust or ionic winds generated by sharp corona electrode tip. *right* Successive time-lapse images indicating the concentration of RBCs near the bottom of the microfluidic chamber toward a stagnation point in a 0.4% hematocrit sample at 286 kV/m and 60 kHz field. Figure reproduced with permission from [31], copyright 2007, American Institute of Physics.



Plasma separation techniques from blood using active energy sources such as acoustophoresis, electrohydrodynamics and dielectrophoresis have also been explored recently [27-33]. Acoustic forces generated by ultrasonic standing waves can be used for plasma separation in microchannels. The radiation force generated on the cells by these acoustic waves moves them into pressure nodes of the standing wave field. By exciting the microfluidic channel with half wavelength width ultrasonic wave, the cells/particles can be focused at the pressure node located at the center of the channel. Thus, pumping blood through the channels, the erythrocytes can be focused at the channel center and removed from the central outlet while the purified plasma can be continuously collected at the side outlets [Figure 2(A)] [27-29]. The device is capable of generating pure fractions of plasma ( $<6 \times 10^6$  cells/mL)

at  $\sim 80 \mu\text{L}/\text{min}$  flow rate. Dielectrophoresis (DEP) offers another effective method of separating blood plasma relying on an inhomogeneous electric field between two electrodes to induce electrostatic forces [Figure 2(B)] to trap cells. When polarizable cells (RBCs) are placed in the non-uniform electric field, a net electric force is imparted on the cells due to an induced or permanent dipole. Separation of blood plasma from diluted blood (1:9) using a DEP microfluidic device was demonstrated by Nakashima *et al.* [33]. Blood is injected into the main channel by capillary force and in the presence of an electric field the RBCs are trapped at the electrodes while cell free plasma is collected downstream. Applying an AC signal of 10 V and 10 MHz, the device is capable of removing about 97% of blood cells to generate 300 nL plasma from 5  $\mu\text{L}$  of blood [33]. Recently, an interesting plasma separation technique based on creating swirling flows in a microfluidic chamber induced by bulk electrohydrodynamics thrust or ionic winds has been reported [Figure 2(C)] [30,31]. Applying a potential that exceeds the threshold ionization voltage for air across a mounted sharp corona electrode tip creates a nearly singular electric field giving rise to a corona discharge. The bulk electrohydrodynamic air thrust generated by the transfer of momentum from collision between the counter-ions with air molecules results in interfacial shear leading to recirculating flows [Figure 2(C)]. The cells suspended in the liquid are thus concentrated towards the bottom of the chamber by these inward radial forces. Using this technique, Yeo and co-workers successfully isolated plasma from RBCs within 200 s applying 0.94 kV voltage and 90 kHz frequency. The separation is efficient with the separated plasma consisting of  $<0.003\%$  hematocrit cell contamination.

### 3. Leukocyte Separation

Leukocytes (or white blood cells (WBCs)) are the nucleated fraction of blood cells, mainly consisting of neutrophils, basophils, eosinophils, monocytes and lymphocytes, and are primarily responsible for all immunological functions. Compared to the vast abundance of erythrocytes ( $\sim 5$  million cells/ $\mu\text{L}$ ), leukocytes are present at a much lower concentration, (typically between 4,000 to 11,000 cells/ $\mu\text{L}$ ) constituting  $\sim 0.1\%$  of all blood cells. Isolation of leukocytes is essential for many hematological analysis and clinical diagnostic tests for monitoring disease progression [34]. Removal of leukocytes from blood, leukapheresis, is essential to reduce the white blood cell count in treating leukemic patients as well as to retrieve blood stem cells in patient with hematologic malignancies [35,36]. It is also essential to remove all leukocytes before performing a blood transfusion to minimize transmission of cell-associated infectious agents (cytomegalovirus, herpes virus, human T-cell lymphoma virus), graft rejection rates and prevent febrile transfusion reactions [37].

Traditionally, these cells are separated from blood by centrifugation exploiting the differences in the buoyant gravity by using a density gradient solution (Ficoll-Paque<sup>TM</sup>). Besides density, leukocytes and RBCs are also structurally different both in terms of shape and size. Leukocytes are spherical nucleated cells with typical diameters ranging from 6  $\mu\text{m}$  to 10  $\mu\text{m}$  [38-40]. Red blood cells (RBCs) on the other hand have a biconcave disc-like structure with an average diameter of 7–8  $\mu\text{m}$  and 2–3  $\mu\text{m}$  thickness. Due to the high deformability of RBCs aided by the absence of nucleus, membrane-based filters are also commonly employed to filter leukocytes from blood [41,42]. The inherent differences in size and deformability between the RBCs and leukocytes have led to the development of several microfluidics techniques based on the principles of cell retention and retarded cell movement [40,43-45].



The use of pillars in particular is an attractive technique for size and deformability based cell sorting in microfluidic devices. For example, Panaro *et al.* designed a silicon microchip with rectangular pillars spaced 3.5  $\mu\text{m}$  to separate leukocytes from whole blood for subsequent PCR reactions [43]. The “deterministic lateral displacement” (DLD) or the “bump array” microdevice developed by Huang *et al.* has also been applied for blood fractionation [Figure 3(A)] [46,47]. The microfluidic device design consists of arrays of micro-pillar structures placed within the main flow channel leading to the formation of multiple cell streams based on size. Cells larger than the critical diameter  $d_c = 20\% \times 2w$  ( $w$  is the separation gap between two adjacent pillars) follow a deterministic path while smaller cells remain unperturbed moving in an average downward flow direction. The bump array was successfully applied for fractionating blood components by tailoring the design to match the sizes of the blood cells. Apart from achieving 110-fold leukocyte enrichment, the device was capable of fractionating the individual WBC components. However, a processing flow rate of 1  $\mu\text{L}/\text{h}$  results in an extremely low device throughput.

A comprehensive study conducted by Ji and coworkers investigated the performance of four main types of silicon microfilter designs, namely, weir-based, membrane, pillars and cross-flow for efficient leukocyte trapping [44]. The critical dimension in all the four microfilter designs was fixed to 3.5  $\mu\text{m}$ . Their results confirm the superiority of the pillars and cross-flow devices for leukocyte trapping with >60% of leukocytes trapped in the device. However, the cross-flow based device outperforms other filter designs in its blood handling capacity (>300  $\mu\text{L}$ ) and allowing >50% of RBCs to pass through. Similar cross-flow based leukocyte separation device have also been reported by other researchers. [40,45]. Sethu *et al.* developed a diffusive filter design consisting of a three parallel channels for leukocyte removal [Figure 3(B)] [40]. The two side channels are connected to the main channel through 2.5  $\mu\text{m}$  deep microfabricated sieves. The sieves allow the passage of >50% deformable RBCs to the side channels while retaining >97% of the larger leukocytes in the center main channel at 5  $\mu\text{L}/\text{min}$  throughput. Recently, VanDelinder and Groisman described a technique to separate cells by size and exchange carrier medium by perfusion in a continuous cross-flow based microfluidic device [45]. By designing 3  $\mu\text{m}$  shallow connecting channels to impede leukocyte migration, the device retains >98% leukocytes in the center channel achieving a remarkably high enrichment factor of 4,000 fold by effectively depleting all RBCs.

While all the aforementioned techniques effectively isolate leukocytes from blood, these techniques commonly suffer from clogging issues leading to shorter operational times and lower throughput. To address these limitations, novel separation techniques taking advantage of the emergent hydrodynamic behavior at the microscale have been developed. Hydrodynamic filtration methods relying on the relative position of the center of the cells in microchannels have been recently demonstrated for separating leukocytes from RBCs [Figure 4(A)] [48,49]. By designing multiple side branching channels, particles/cells of varying diameter can be aligned along the channel sidewalls and collected at different outlets downstream [48]. The device reports a ~29 fold leukocyte enrichment at a relatively high flow rate of 20  $\mu\text{L}/\text{min}$  with no clogging. Similarly, the device developed by Zheng *et al.* takes advantage of the position of the leukocytes and RBCs along the flow streamlines to separate them in different outlets [49]. As the center of the leukocytes is further away from the channel sidewalls than the smaller RBCs, this allows the leukocytes to be extracted at outlets placed further downstream with a high separation efficiency of >97%. Another novel separation technique based on the principle of



hydrophoresis has been reported for leukocyte isolation in microchannels patterned with slanted grooves on the top and bottom channel walls [50]. The hydrodynamic interaction of cells with a fluid flow induced by slant obstacles forces them to flow in different trajectories depending on the cell diameter. Using diluted blood (1:20), the device demonstrates a 210 fold leukocyte enrichment with 85% recovery at a processing throughput of 4,000 cells/s.

**Figure 3.** Leukocytes separation from blood. (A) *left*: Schematic of the fractionating device used for separating blood components based on deterministic lateral displacement (DLD) technique. *centre* Graphic illustrating the DLD separation principle together with histogram showing concentrations of different blood leukocyte components collected at the three outlets after separation. *right*: Experimental images showing the displacement of the bigger leukocytes (labeled with Hoechst 33342 dye) away from the inlet sample stream towards the right side of the channel by the bump array. Reprinted with permission from [47], copyright 2006 National Academy of Sciences, USA; (B) *left*: Schematic of the diffusive filter based microdevice for continuous flow fractionation of leukocytes from whole blood based on size and shape differences. The microchannel design consists of three parallel channels connected by 2.5 μm deep micro sieves. Blood pumped through the main channel center is depleted of RBCs at the side channels by cross-flow filtration while the bigger leukocytes are retained at the centre channel. *right*: Histogram showing the experimental fractionation results as a function of flow rate. At an optimal flow rate of 5 μL/min >97% of leukocytes are collected from the center outlet with 50% RBC depletion. Redrawn with permission from [40], copyright 2006, The Royal Society of Chemistry.

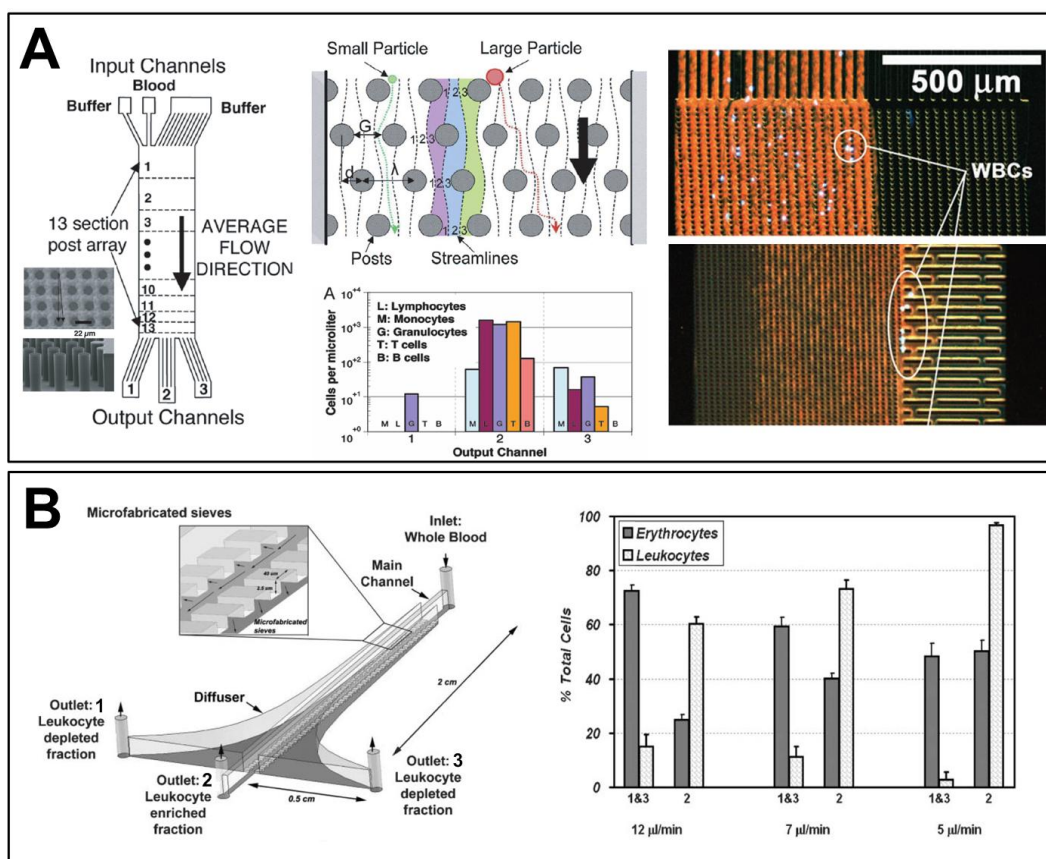
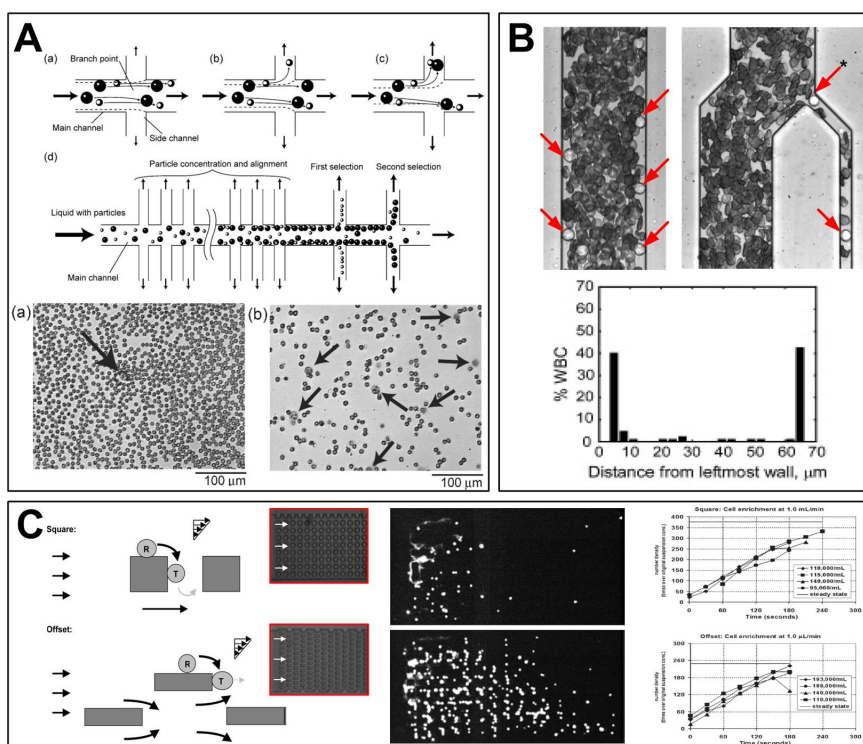


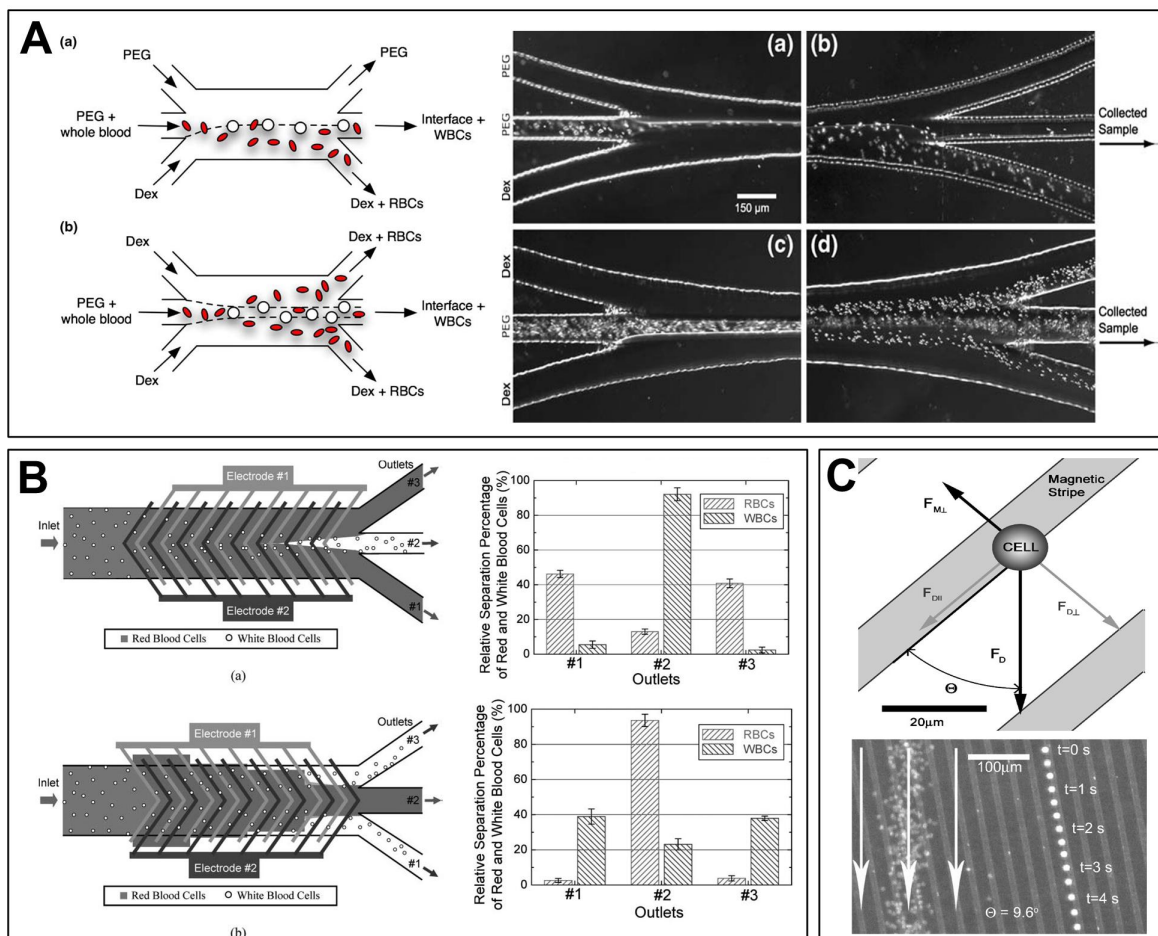
**Figure 4.** (A) *top*: Leukocyte separation using hydrodynamic filtration. Schematic diagrams showing the particle position and trajectory at a branch point for low, medium, and high relative flow rates between the main and side channels. As liquid is continuously withdrawn from the side channels, all particles concentrate along the channel sidewalls and are separated into multiple side channels based on size. *bottom*: Microscopic images showing enrichment of leukocytes (indicated by arrows) before filtration (a) and at outlet 1 and 3 after second filtration (b). Figure reproduced with permission from [48], copyright 2005, The Royal Society of Chemistry; (B) Biomimetic leukocyte separation technique based on *in vivo* leukocyte margination phenomenon. *top*: The larger WBCs (red arrows) are displaced to the channel sidewalls due to axial migration of RBCs and extracted using an asymmetrically bifurcated outlet as shown. *bottom*: Histogram showing the leukocyte distribution at the end of a 5.5 mm long rectangular microchannel indicating the successful margination of all the leukocytes towards the channel side accomplishing a 34-fold enrichment. Figure redrawn with permission from [51], copyright 2005, American Chemical Society; (C) Affinity capture of leukocytes using patterned microstructures based on leukocyte recruitment and rolling. *left*: Illustration of different stages of cell adhesion in the square and offset micropillar array. As cells adhere on the lateral surface of the E selectin coated pillars (R), the fluid shear in the tangential direction make the cells roll along the pillars. Reaching the end of the pillars, these cells tend to tether and detach from the surface before being captured again by an adjacent pillar. Insets (red box) shows the microchannel image with square and offset arrays. *centre*: Images showing the accumulation of HL-60 cells captured along the square array at the start (top) and 2 min later (bottom). *right*: Graph showing the enrichment of HL-60 cells with time. HL-60 cells were enriched ~400 times in the square array and ~240 times in the offset array. Figure reprinted with kind permission from [53], copyright 2005, The Royal Society of Chemistry.



*In vivo* physiological phenomenon such as leukocyte margination and recruitment in the microcirculation has also been mimicked in microfluidic devices for leukocyte separation [51-53]. In blood vessels with luminal diameter less than 300  $\mu\text{m}$ , RBCs due to their smaller size and higher deformability than the leukocytes, tend to migrate to the axial centre of the vessel under Poiseuille flow conditions. As these RBCs migrate towards the axial centre, mechanical collisions between the leukocytes and the migrating RBCs results in the displacement of the larger leukocytes towards the vessel wall; a phenomenon termed as margination [52,54]. This bio-mimetic phenomenon can be exploited to achieve  $\sim 34$  fold leukocyte enrichment by designing appropriately branched daughter channels to continuously filter all the leukocytes present along the microchannel sidewalls from blood [Figure 4(B)] [51]. Recently, separation of leukemic HL-60 and U-937 cells based on the interaction between the cells and protein coated microchannel surfaces has also been demonstrated [Figure 4(C)] [53]. By coating pillar surfaces with E-selectin adhesion proteins to mimic *in vivo* phenomenon of leukocyte recruitment, the leukemic cells are immuno-captured and arrested from the passing flow. Due to the high selectivity, this technique permits the capture of  $>95\%$  cells with 150-fold average enrichment at a throughput of 15,000 cells/min.

Most of the above mentioned techniques separate leukocytes based on their mechanical properties such as size and deformability. Besides taking advantage of the differences in these distinct mechanical properties to sort leukocytes from RBCs, the varying surface properties and net charges of these cells can also be used for efficient sorting as well. For example, SooHoo and Walker developed a novel method to separate leukocytes from whole blood using microfluidic aqueous two-phase system (ATPS) [Figure 5(A)] [55]. Using a three inlet system, polyethylene glycol (PEG) and dextran (Dex) solution are used to create one or two immiscible interfaces inside the microchannel. Blood diluted in PEG (1:50) is pumped through the center inlet, with dextran solutions pumped through the two side inlets. The PEG-Dex interface exhibits a force on the cells due to the ATPS interface surface energy. The magnitude of this force is proportional to the surface area and thus the leukocytes having a larger surface area experience higher force and prefer being at the interface while the RBCs migrate into the dextran solution. This simple separation method can process diluted blood at 1  $\mu\text{L}/\text{min}$  flowrate with a  $\sim 10$  fold leukocyte enrichment with a two interface design [55]. Another interesting leukocyte recovery method taking advantage of the difference in lysing time between the leukocytes and RBCs when mixed in a hypotonic solution (de-ionized water) has been explored. When mixed with de-ionized water, RBC lysis completes within 8 s while leukocyte lysis begins after 3 s [56]. By designing a 3-inlet microfluidic cassette (side inlets pump de-ionized water) integrated with a micromixer for efficient mixing and controlling the exposure time to within 10 s, all leukocytes are recovered along with the lysed RBC debris at the outlet [56].

**Figure 5.** (A) *left*: Schematic illustration of leukocyte separation based on microfluidic aqueous two-phase system (ATPS). Whole blood diluted in PEG is exposed to either a one or two PEG-Dex interfaces, represented by the *dashed line*. Due to differences in surface energies, the leukocytes prefer the interface while RBCs migrate into the Dex region. *right*: Experimental images showing leukocyte separation from blood in one interface PEG-PEG-Dex system (a-b) and two interfaces Dex-PEG-Dex system (c-d). Figure reprinted from [55], copyright 2009, with permission from Springer Science + Business Media, LLC; (B) *left*: Schematic representation of lateral driven continuous dielectrophoretic separators using an (a) divergent and (b) convergent type interdigitated electrode pattern. *right*: Histograms showing the relative separation percentage of RBCs and WBCs at each outlet using the divergent (top) and convergent (bottom) type DEP microseparators. Figure reproduced with permission from [57], copyright 2008, The Royal Society of Chemistry; (C) *top*: Diagram showing various forces acting on a magnetically labeled cell passing over a magnetic stripe. By incubating blood with super paramagnetic CD45 microbeads, the flow trajectory of leukocytes can be altered by the magnetic stripes. *bottom*: Time lapse image showing a single tagged fluorescent leukocyte tracking along a magnetic stripe inclined at an angle of  $9.6^\circ$  to the fluid flow, indicated by white arrows. The RBCs in blood continue to remain in the sample stream and are unaffected by the magnetic force. Figure reproduced with permission from [58], copyright 2004, American Institute of Physics.



Leukocyte separation using active sorting techniques including dielectrophoresis and magnetic separation have been reported recently on the microscale. Han *et al.* developed lateral-driven dielectrophoretic (DEP) microseparators to isolate leukocytes from blood suspended in a highly conductive medium [Figure 5(B)] [57]. By subjecting the blood cells to a constant dielectrophoretic forces generated using patterned convergent and divergent type interdigitated microelectrodes, the leukocytes were separated from RBCs. As the RBCs have a higher density compared to leukocytes (RBCs  $\sim 1,130 \text{ kg.m}^{-3}$ , WBCs  $\sim 1,050\text{--}1,080 \text{ kg.m}^{-3}$ ), the DEP force acting on them is higher resulting in a larger deflection at the electrodes. The authors report a 92% leukocyte recovery with  $\sim 7$  fold enrichment at a continuous flow rate of  $50 \mu\text{L/h}$ . Finally, magnetic based leukocyte separation methods exploiting either inherent differences in the cells magnetic susceptibility or selectively immuno-labeling magnetic beads have been demonstrated [58-61]. For example, whole blood incubated with CD45 labeled super paramagnetic microbeads pumped through a microchannel with patterned magnetic stripes has been explored for leukocyte isolation [Figure 5(C)] [58]. As all leukocytes express CD45 surface markers to some degree, the magnetic stripes (magnetized by an externally applied field of 0.08T) alter the flow direction of the CD45 tagged leukocytes from unlabeled cells, thus achieving separation. Although, the selectivity of this technique is very high due to immuno-labeling, a significant portion ( $\sim 50\%$ ) of leukocytes were lost either by being permanently stuck to the magnetic strips or were not sufficiently magnetized to alter their direction [59]. Additionally, magnetic bead sorting often requires pre-treatment of cells, which may damage cells inadvertently. To overcome this problem, separation of RBCs from leukocytes based on the inherent magnetic susceptibility of these cells has also been reported [60,61]. By patterning a ferromagnetic wire within a microchannel the wire concentrates and attracts the paramagnetic RBCs along its length while the diamagnetic leukocytes are separated in a continuous and efficient manner [61]. Using a three-stage cascaded system, the authors report a 97% leukocyte recovery with  $15\times$  enrichment at moderate flow rates of  $2.5\text{--}20 \mu\text{L/h}$  [61].

#### 4. Platelet Separation

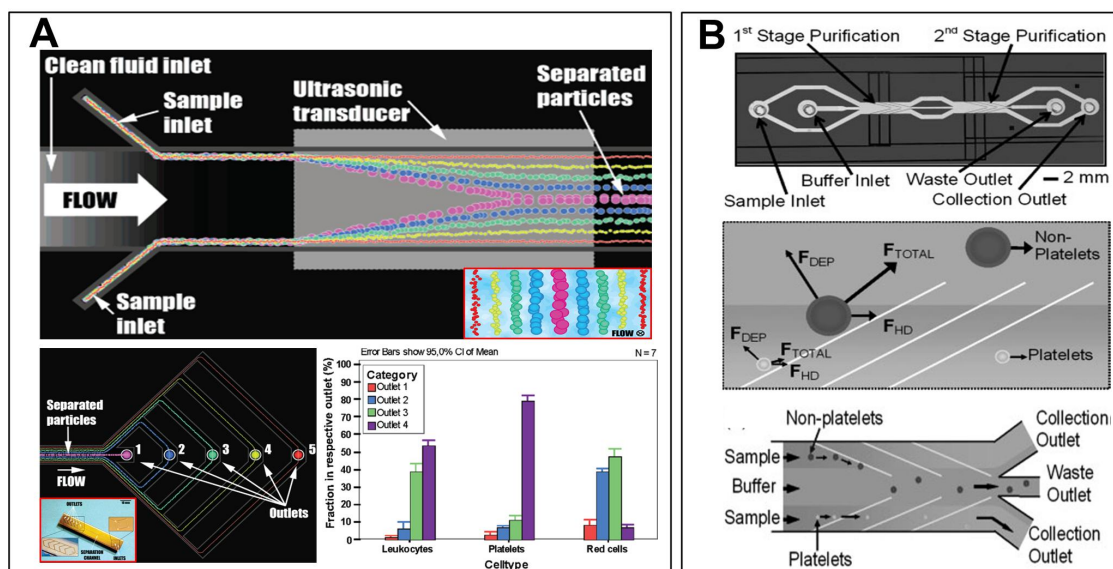
Platelets are the smallest type of cells found in blood ( $\sim 2\text{--}3 \mu\text{m}$  diameter), and they are involved in many fundamental physiological processes such as hemostasis and thrombosis [62]. When bleeding from a wound occurs, circulating platelets adhere and aggregate at the injury site to initiate thrombus formation until the bleeding is stopped. Patients undergoing general surgery, organ transplants and trauma treatments frequently require platelet transfusion [63]. Platelets are usually extracted from blood via centrifugation and by other methods which include platelet-rich plasma preparation (PRP), the buffy-coat preparation (BC) and apheresis [64]. However, these techniques are inefficient because a significant portion of inactivated platelets are often lost either through high mechanical shear stress [65] or the purification process directly [64]. Thus new efforts in developing efficient platelets extraction are leveraging on existing low stress microfluidic technologies.

Platelet separation in microfluidic systems has mainly been explored with active separation techniques using acoustophoresis [66] and dielectrophoresis [67]. Platelets can be separated into multiple fractions in a continuous mode via free flow acoustophoresis (FFA) [Figure 6(A)] [66]. A half-wavelength acoustic standing wave generated between the microchannel side walls applies an



acoustic radiation force perpendicular to the direction of the flow. By using a combination of FFA and medium density manipulation, high separation efficiency can be achieved with 92% of the erythrocytes ending in the first fraction (center of the channel) while 99% of the platelets collected in the second. Similarly, by exploiting the fact that platelets are the smallest cells in blood and therefore experiences less dielectrophoretic force, dielectrophoresis can be used to extract high purity platelets (~95%) from diluted whole blood at a throughput of  $\sim 2.2 \times 10^4$  cells/s with minimal platelet activation [Figure 6(B)] [67]. Recently, single-step separation of individual platelets from whole blood by micropatterning of platelet-specific protein surfaces on solid substrates has been reported using an interfacial platelet cytometry (iPC) chip [62]. Platelets were separated from whole blood using iPC coated with fibrinogen, von Willebrand factor (VWF), and anti-CD42b antibody printed “spots” ranging from 2–24  $\mu\text{m}$  diameter. The paper reports on tests conducted with blood samples from healthy donors and a Glanzmann’s Thrombasthenia patient. As the platelets are allowed to adhere to the surface, the iPC chip enables physiologically relevant platelet bioassays based on platelet/protein-matrix interactions.

**Figure 6.** Platelets separation from blood. (A) *top*: Illustration of free flow acoustophoresis (FFA) showing size-based separation of particles or cells into multiple fractions in a continuous flow manner. The varying acoustic forces equilibrate the larger cells closer to the channel center and smaller cells farther from the center. *bottom*: The fractionated particles can be collected separately by designing five consecutive outlets/fractions. The histogram shows the separation of platelets, RBCs and leukocytes at the various outlets indicating majority of platelets collected at outlet 4. Reprinted with kind permission from [66], copyright 2007, American Chemical Society; (B) *top*: Device architecture of the two-stage DEP-activated cell sorter (DACS) chip. The integration of two tandem purification stages increases the purity of the platelet population at the collection outlet. *bottom*: Schematic illustration of the DEP separation principle indicating the forces acting on the blood cells. The larger blood cells experience a higher DEP force from the electrodes and are deflected from the side to the central buffer stream while the smaller platelets are a retained in the side buffer stream. Figure adapted with permission from [67]. copyright 2008 Wiley-VCH Verlag GmbH and Co. KGaA.



## 5. Rare-Cell Separation

Besides blood constituents, other cells of interest such as circulating tumor cells (CTCs), nucleated RBCs (nRBCs) and microorganisms are also present in peripheral blood, which are of clinical significance and important for disease diagnosis and fundamental research. As these cells usually occur in low abundance ( $\sim 1\text{--}10,000$  cells/ mL of blood ( $\sim 10^9$  RBCs)), common macroscale separation techniques such as physical filtration, fluorescence-activated cell sorting (FACS) and magnetically-actuated cell sorting (MACS) have limited success in separating/isolating them mainly due to laborious sample preparations which introduce artifacts or lead to loss of desired cells [68]. Moreover, mechanical stress-induced changes in original cell phenotype using these techniques have also been reported, suggesting the need to develop new tools for separating these rare cells [69,70]. Microfluidic based separation methods are an attractive alternative due to the small length scale and numerous advantages such as reduced sample and reagent volumes, minimize contamination issues and process automation [4,34]. These inherent advantages also make microfluidics ideal in resource-poor settings where problems such as shortage of power supply and refrigeration are limiting the use of expensive and specialized equipment. For example, several microfluidic devices have been developed for malaria detection, which is one of the severest parasitic blood-borne diseases and most prevalent in the poorer countries. The separation principles are mostly based on intrinsic properties of malaria-infected RBCs (*i*RBCs) such as dielectric differences [71], paramagnetic affinity [72], and change in stiffness [73,74] to separate or enrich them from blood for diagnostic applications. However, as *i*RBCs constitute  $\sim 0.01\text{--}1\%$  in peripheral blood of malaria patients, they are not considered as rare-cell per se and thus excluded in our discussion. In this section, separation of various types of rare cells from blood using microfluidics will be presented.

### 5.1. Nucleated RBCs

Prenatal diagnosis for genetic abnormalities in fetus is usually performed by collecting fetal samples through amniocentesis and chorionic villus sampling (CVS), which are invasive procedures and puts the patient at risk of miscarriage. While ultrasonography and serum biochemistry testing are currently used to screen patients for non invasive prenatal diagnosis, it has been reported fetal nucleated RBCs (nRBCs) present in maternal circulation can be used for direct analysis of fetal chromosomes and their enumeration is also associated with fetal aneuploidies or pregnancy complications [75,76]. In addition, nRBCs have short life span and are unlikely to persist between pregnancies, making them a suitable candidate for direct fetal karyotype analysis. As nRBCs are extremely rare ( $\sim 1\text{--}30$  nRBCs/mL of blood), enrichment or isolation of these cells usually consists of density gradient centrifugation to obtain the mononuclear cells, followed by immuno-labeling and FACS or MACS selection. These procedures are time consuming, labor-intensive and leads to significant loss of nRBCs.

Several microfluidics devices have been developed to isolate these nRBCs using intrinsic markers such as size and deformability, and hemoglobin content. The nRBCs are around  $9\text{--}12\ \mu\text{m}$  and similar in size with leukocytes ( $10\text{--}15\ \mu\text{m}$ ), but larger than bulk of the RBCs ( $\sim 6\text{--}8\ \mu\text{m}$  in diameter). Mohamed *et al.* have developed a simple microdevice which consists of an array of micropillars of



different gap sizes (2.5 to 15  $\mu\text{m}$ ) to separate the fetal nRBCs from blood based on size and deformability [Figure 7(A)] [77]. Using mononuclear cells as their sample, they demonstrated that all the leukocytes were trapped at the 2.5  $\mu\text{m}$  width gaps while nRBCs deformed through the entire device and were collected for subsequent DNA analysis. No immunolabeling was required in this process but sample preparation including sample dilution and ficoll centrifugation were used to obtain the mononuclear layer. The device throughput was also considerably low ( $\sim 0.35$  mL/h) taking  $\sim 6$ – $8$  h to process each sample. To improve the throughput, Lee *et al.* have recently developed a microfluidic device which continuously separates nRBCs from RBCs based on cross-flow filtration [78]. In this system, sample and buffer solutions were pumped into the bottom and upper inlet respectively. Smaller RBCs were filtered through the inclined filter of 4  $\mu\text{m}$  gap and collected at the bottom outlet (port 4). The bigger nRBCs, which could not deform through, would roll along the filter and be diverted upstream into the upper outlet (port 3), thus achieving separation. Throughput was higher in this device (0.3 mL/min) with good nRBCs recovery (74%), while 46.5% of RBCs were depleted in the upper outlet ( $\sim 1.7$  fold enrichment). However, a major limitation was the absence of whole blood testing, in which the bigger and stiffer leukocytes would probably clog the filters or be diverted upstream, resulting in lower nRBCs purity. Moreover, in both aforementioned methods, only dilute blood samples could be used as RBCs clog the filters easily which would affect the separation efficiency of nRBCs.

Recently, Huang *et al.* developed a 2-step microfluidic based isolation technique for nRBCs using the popular ‘deterministic lateral displacement’ phenomenon [79]. In the first step, using the bump array microchip, the larger leukocytes and nRBCs were separated from the RBCs and platelets. Post sorting, the mononuclear cells (nRBCs and leukocytes) were treated with sodium nitrite to convert the hemoglobin present in nRBCs to methemoglobin which is paramagnetic in nature allowing the isolation of nRBCs using a magnetic column. This microfluidic-magnetic combination method was able to eliminate 99.99% RBCs and leukocytes with 100% nRBCs identification in 58 predetermined samples [79]. Throughput was also higher in this device ( $\sim 2.5$  mL/h) and whole blood was used directly without sample dilution. Further work will be necessary to integrate both processes into a single device to improve nRBCs isolation from blood for non invasive prenatal diagnosis.

## 5.2. Circulating Tumor Cells

Circulating tumor cells (CTCs) in blood is an important intermediate step in cancer metastasis, which accounts for  $\sim 90\%$  of all cancer related deaths [80]. Clinical studies have shown that enumeration of CTCs can be correlated with cancer progression [81,82] and this “liquid biopsy” is more practical as they can be performed more frequently than traditional invasive biopsies to predict prognosis and guide therapy in cancer patients [83,84]. For CTCs enumeration to be useful in clinical management of cancer, a highly efficient and robust CTC separation tool is required due to the low abundance of these CTCs in blood. In the past decade, several microfluidics platforms have been developed for CTCs separation from blood based on either physical filtration or affinity capture.

Due to the large size differences between CTCs and other blood cellular components (CTCs  $\sim 16$ – $20$   $\mu\text{m}$ ; RBC  $\sim 8$   $\mu\text{m}$ ; leukocytes  $\sim 10$ – $15$   $\mu\text{m}$ ) [85,86], size-based CTCs separation in microfluidic devices is often achieved using microstructures of different geometries to physically trap the larger CTCs [87-90]. The critical dimension in these devices is the size of the pore/structure which is designed to allow

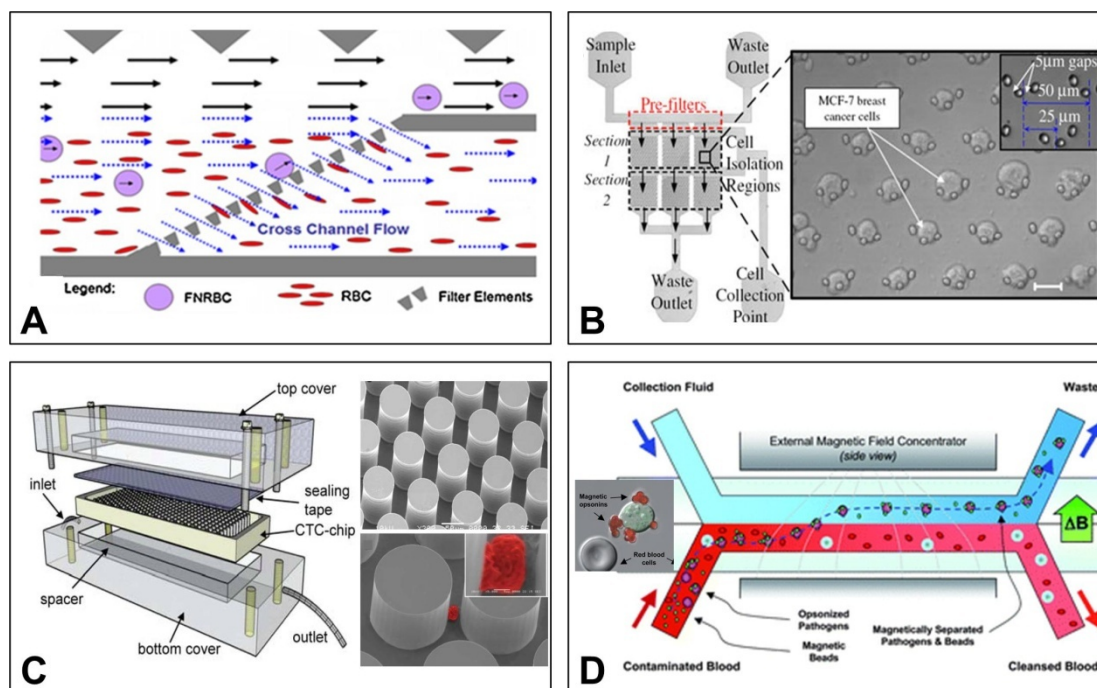
maximum CTCs trapping with little contamination. Using gap sizes between 5 to 10  $\mu\text{m}$ , these microfluidic devices are able to demonstrate isolation of cancer cells with high efficiency (>80%), but the isolation purity varies greatly due to trapping of the bigger leukocytes [87-89]. The trapped CTCs usually deforms at the pores under constant shear during sample processing, making their retrieval difficult and thus requiring post-sorting analysis to be done on chip. To address this problem, Tan *et al.* used an array of crescent-shaped isolation traps to isolate the CTCs in a more gentle manner which allowed subsequent retrieval out of chip for downstream analysis [Figure 7(B)] [90]. The separation principle is simple, does not require the use of biomarkers like EpCAM anti-bodies and allow the retrieval of viable CTCs for further molecular characterization and analysis.

Apart from physical filtration methods, affinity based capture of CTCs in microfluidic devices either by immobilizing specific capture molecules on magnetic beads [91], microstructures [92,93], or array of channels [94] has been a popular CTC isolation approach. Using an array of anti EpCAM-coated microposts, Nagrath *et al.* demonstrated that they were able to isolate CTCs from peripheral blood in 115 out of 116 (~99%) cancer patients in a single step [Figure 7(C)] [93]. However, a major drawback for affinity capture is difficulty in finding ligands that have high specificity and affinity for CTCs due to their heterogeneity in surface molecular signatures. The use of common epithelial markers such as EpCAM is less desirable as EpCAM expression varies widely for different or even same tumor type [95] and retrieval of isolated CTCs may be difficult due to cell binding in the devices. Moreover, there is a risk of losing the most aggressive CTCs subpopulation due to epithelial to mesenchymal transition (EMT) process, which leads to a down-regulation of epithelial surface markers and thus the inability for CTCs to bind efficiently [96,97]. Recently, it has been demonstrated that aptamers (single-stranded nucleic acid oligomers) could be used as probes to isolate CTCs with high affinity and specificity [98,99]. As aptamers are synthesized by an *in vitro* process known as cell-SELEX (Systematic Evolution of Ligands by EXponential enrichment), the surface molecular information of CTCs are not required and different aptamer probes can be generated for any type or subpopulation of CTCs. Whole blood can be used directly without dilution for affinity capture, but throughput is still slow due to low shear rates to allow sufficient time for the CTCs to bind to capture surfaces as well as to prevent bound CTCs from being detached under high shear.

### 5.3. Microorganisms

Separation of microorganisms from blood is primarily used as a therapeutic blood cleansing method for treating sepsis, a lethal disease caused by a systemic microbial infection that spreads via the bloodstream and compromise the body's immunological system [100]. Antibiotics are often the main course of treatment, but inflammation continues to spread for a few hours before the drugs are effective. For newborn infants with sepsis (neonatal sepsis), their immune system are still functionally immature and delay or inappropriate antibiotic treatment may cause fatality [101]. In this section we will review several microfluidic technologies which have been developed to separate microorganisms and pathogens from blood for potential sepsis treatment.

**Figure 7.** Rare cells separation from blood using microfluidics. **(A)** Schematic of the cross flow filtration principle for nRBCs separation. RBCs are continuously filtered out through the inclined filters with a 4  $\mu\text{m}$  gap while the bigger nRBCs cannot deform through the filters and are made to roll along the filter upstream and collected separately. Figure reprinted from [78], copyright 2010, with kind permission from Elsevier; **(B)** Schematic design of a microfluidic device for CTCs isolation and enumeration. Placing crescent-shaped cell traps in the isolation regions traps the larger tumor cells while allowing smaller blood components to sieve through. Figure reproduced from [90], copyright 2009, with permission from Springer Science + Business Media, LLC; **(C)** Layout of the CTC chip designed by Nagrath *et al.* consisting of functionalised micropost array for affinity capture of CTCs. Inset showing a scanning electron micrograph of a lung cancer cell captured between two microposts. Reprinted with permission from Macmillan Publishers Ltd: Nature [93], copyright 2007; **(D)** Schematic illustrating the separation principle using a micromagnetic-microfluidic based blood cleansing device to selectively remove pathogens from contaminated blood. Immunomagnetic microbeads bind selectively to the pathogens (see inset) to create magnetic opsonins which are removed continuously in the presence of magnetic field gradients. Figure adapted with permission from [105], copyright 2009, The Royal Society of Chemistry.



Typically microorganisms are very small ranging from 1 to 3  $\mu\text{m}$  in diameter and thus can be easily separated from the larger RBCs and leukocytes. Wu *et al.* separated bacteria from blood using inertial lift force-induced migration based on size difference between bacteria and blood cells [102]. The technique relies on the lateral displacement of the larger RBCs due to stronger wall-induced inertial lift forces while the bacteria would remain in sample stream. The authors demonstrated removal of ~60% bacteria from a 10% (v/v) blood samples at a flow rate of 18  $\mu\text{L}/\text{min}$ . Using similar inertial focusing principle, Mach *et al.* developed a high throughput blood filtration device which consists of

40 high-aspect-ratio channels in parallel that can filter out bacteria from diluted blood sample (0.5% hematocrit) at 8 mL/min continuously [103]. As inertial separation relies entirely on intrinsic hydrodynamic forces, the design and device fabrication of these devices is simple and the large channel dimensions also eliminate problems of channel clogging [4]. However, cell–cell interactions can deteriorate the efficiency of this separation technique whereby only dilute samples can be used, thus requiring additional sample preparation procedures.

Recently micromagnetic based microfluidic blood cleansing have been developed by Xia and co-workers. The design consists of a microfluidic “H-filter” for continuous separation of E-coli from blood using magnetic nanoparticles specifically bound to bacteria [Figure 7(D)] [104]. By fabricating a magnetic (NiFe) microcomb structure adjacent to the channel, a steep magnetic field gradient can be generated across the flow channel when magnetised externally allowing the opsonized bacteria to be deflected from the original flow path and collected separately. The group demonstrated a throughput of  $\sim 10^4$  cells/sec (at flow rates of 25  $\mu$ L/h) with bacteria separation efficiency of  $\sim 78\%$  using whole blood sample spiked with *E coli*. The group later improved the design using an array of channels and demonstrated fungal separation from whole blood with 1000 $\times$  higher throughput ( $\sim 20$  mL/h) [105]. This method is highly versatile and can be used to separate multiple types of infectious microorganisms simultaneously by using appropriately labeled magnetic beads. However, one would require prior information on the pathogens to select the binding molecules for coating of magnetic beads.

## 6. Conclusions and Outlook

Here, we highlight the development of several microfluidic approaches that exploit the different physical characteristics of cells, fluid mechanics and biorheology of blood as well as the difference in binding affinity of specific targeted cells to separate and/or enrich them. These include red cells, leukocytes, platelets, rare cells (such as CTCs) and pathogens (such as bacteria).

We envisage that we will continue to push the boundary of this research as more creative and innovative methods continue to be developed and introduced in the near future. It is likely that they will cater not only for the processing of both large and small volumes of blood, but are also fast and efficient and with high sensitivity, purity and yield. However, for these blood-based separation systems to be realized as true point-of-care (POC) devices, these techniques and devices must be simple, easy to use and with little or no sample preparation required. This will set the challenges for researchers working on POC devices and will by no means be easy, but possible.

## References and Notes

1. Whitesides, G.M. The origins and the future of microfluidics. *Nature* **2006**, *442*, 368-373.
2. Squires, T.M.; Quake, S.R. Microfluidics: Fluid physics at the nanoliter scale. *Rev. Mod. Phys.* **2005**, *77*, 977-1026.
3. Toner, M.; Irimia, D. Blood-on-a-chip. *Annu. Rev. Biomed. Eng.* **2005**, *7*, 77-103.
4. Bhagat, A.A.S.; Bow, H.; Hou, H.W.; Tan, S.; Han, J.; Lim, C.T. Microfluidics for cell separation. *Med. Biol. Eng. Comput.* **2010**, *48*, 999-1014.
5. Pamme, N. Continuous flow separations in microfluidic devices. *Lab Chip* **2007**, *7*, 1644-1659.

6. Kersaudy-Kerhoas, M.; Dhariwal, R.; Desmulliez, M.P.Y. Recent advances in microparticle continuous separation. *IET Nanobiotechnol.* **2008**, *2*, 1-13.
7. Eijkel, J.C.T.; van den Berg, A. Nanotechnology for membranes, filters and sieves. *Lab Chip* **2006**, *6*, 19-23.
8. Tsutsui, H.; Ho, C.M. Cell separation by non-inertial force fields in microfluidic systems. *Mech. Res. Commun.* **2009**, *36*, 92-103.
9. Kulrattanak, T.; van der Sman, R.G.M.; Schroen, C.; Boom, R.M. Classification and evaluation of microfluidic devices for continuous suspension fractionation. *Adv. Colloid Interface Sci.* **2008**, *142*, 53-66.
10. Azim, W.; Azim, S.; Ahmed, K.; Shafi, H.; Rafi, T.; Luqman, M. Diagnostic significance of serum protein electrophoresis. *Biomedica* **2004**, *20*, 40-44.
11. Kagan, B.M. The clinical significance of the serum protein's. *South. Med. J.* **1943**, *36*, 234.
12. Haeberle, S.; Brenner, T.; Zengerle, R.; Dürée, J. Centrifugal extraction of plasma from whole blood on a rotating disk. *Lab Chip* **2006**, *6*, 776-781.
13. Lai, S.; Wang, S.; Luo, J.; Lee, L.J.; Yang, S.T.; Madou, M.J. Design of a compact disk-like microfluidic platform for enzyme-linked immunosorbent assay. *Anal. Chem.* **2004**, *76*, 1832-1837.
14. Wong, A.P.; Gupta, M.; Shevkoplyas, S.S.; Whitesides, G.M. Egg beater as centrifuge: Isolating human blood plasma from whole blood in resource-poor settings. *Lab Chip* **2008**, *8*, 2032-2037.
15. Brody, J.P.; Osborn, T.D.; Forster, F.K.; Yager, P. A planar microfabricated fluid filter. *Sens. Actuat. A* **1996**, *54*, 704-708.
16. VanDelinder, V.; Groisman, A. Separation of plasma from whole human blood in a continuous cross-flow in a molded microfluidic device. *Anal. Chem.* **2006**, *78*, 3765-3771.
17. Crowley, T.A.; Pizziconi, V. Isolation of plasma from whole blood using planar microfilters for lab-on-a-chip applications. *Lab Chip* **2005**, *5*, 922-929.
18. Lin, L.; Guthrie, J.T. Preparation and characterisation of novel, blood-plasma-separation membranes for use in biosensors. *J. Membr. Sci.* **2000**, *173*, 73-85.
19. Moorthy, J.; Beebe, D.J. *In situ* fabricated porous filters for microsystems. *Lab Chip* **2003**, *3*, 62-66.
20. Shim, J.S.; Browne, A.W.; Ahn, C.H. An on-chip whole blood/plasma separator with bead-packed microchannel on COC polymer. *Biomed. Microdevices* **2010**, *12*, 949-957.
21. Yang, S.; Undar, A.; Zahn, J.D. A microfluidic device for continuous, real time blood plasma separation. *Lab Chip* **2006**, *6*, 871-880.
22. Yang, S.; Ji, B.; Ündar, A.; Zahn, J.D. Microfluidic devices for continuous blood plasma separation and analysis during pediatric cardiopulmonary bypass procedures. *ASAIO J.* **2006**, *52*, 698.
23. Fan, R.; Vermesh, O.; Srivastava, A.; Yen, B.K.H.; Qin, L.D.; Ahmad, H.; Kwong, G.A.; Liu, C.C.; Gould, J.; Hood, L.; *et al.* Integrated barcode chips for rapid, multiplexed analysis of proteins in microliter quantities of blood. *Nat. Biotechnol.* **2008**, *26*, 1373-1378.
24. Jaggi, R.D.; Sandoz, R.; Effenhauser, C.S. Microfluidic depletion of red blood cells from whole blood in high-aspect-ratio microchannels. *Microfluid. Nanofluid.* **2007**, *3*, 47-53.
25. Blatter, C.; Jurischka, R.; Schoth, A.; Kerth, P.; Menz, W. Separation of blood cells and plasma in microchannel bend structures. *Proc. SPIE* **2004**, *5591*, 143-151.

26. Blattert, C.; Jurischka, R.; Tahhan, I.; Schoth, A.; Kerth, P.; Menz, W. Separation of blood in microchannel bends. *Proc. SPIE* **2004**, *26*, 2627-2630.
27. Lenshof, A.; Ahmad-Tajudin, A.; Jaras, K.; Sward-Nilsson, A.M.; Aberg, L.; Marko-Varga, G.; Malm, J.; Lilja, H.; Laurell, T. Acoustic whole blood plasmapheresis chip for prostate specific antigen microarray diagnostics. *Anal. Chem.* **2009**, *81*, 6030-6037.
28. Petersson, F.; Nilsson, A.; Holm, C.; Jönsson, H.; Laurell, T. Separation of lipids from blood utilizing ultrasonic standing waves in microfluidic channels. *Analyst* **2004**, *129*, 938-943.
29. Petersson, F.; Nilsson, A.; Holm, C.; Jönsson, H.; Laurell, T. Continuous separation of lipid particles from erythrocytes by means of laminar flow and acoustic standing wave forces. *Lab Chip* **2005**, *5*, 20-22.
30. Yeo, L.Y.; Friend, J.R.; Arifin, D.R. Electric tempest in a teacup: The tea leaf analogy to microfluidic blood plasma separation. *Appl. Phys. Lett.* **2006**, *89*, 103516.
31. Arifin, D.R.; Yeo, L.Y.; Friend, J.R. Microfluidic blood plasma separation via bulk electrohydrodynamic flows. *Biomicrofluidics* **2007**, *1*, 014103.
32. Xu, C.X.; Wang, Y.; Cao, M.; Lu, Z.H. Dielectrophoresis of human red cells in microchips. *Electrophoresis* **1999**, *20*, 1829-1831.
33. Nakashima, Y.; Hata, S.; Yasuda, T. Blood plasma separation and extraction from a minute amount of blood using dielectrophoretic and capillary forces. *Sens. Actuat. B* **2010**, *145*, 561-569.
34. Pratt, E.D.; Huang, C.; Hawkins, B.G.; Gleghorn, J.P.; Kirby, B.J. Rare cell capture in microfluidic devices. *Chem. Eng. Sci.* **2010**, *66*, 1508-1522.
35. Buckner, D.; Graw, R.G., Jr.; Eisel, R.J.; Henderson, E.S.; Perry, S. Leukapheresis by continuous flow centrifugation (CFC) in patients with chronic myelocytic leukemia (CML). *Blood* **1969**, *33*, 353.
36. Malachowski, M.E.; Comenzo, R.L.; Hillyer, C.D.; Tiegerman, K.O.; Berkman, E.M. Large volume leukapheresis for peripheral blood stem cell collection in patients with hematologic malignancies. *Transfusion* **1992**, *32*, 732-735.
37. Chu, R.W. Leukocytes in blood transfusion: Adverse effects and their prevention. *Hong Kong Med. J.* **1999**, *5*, 280-284.
38. Schmid-Schonbein, G.W.; Shih, Y.Y.; Chien, S. Morphometry of human leukocytes. *Blood* **1980**, *56*, 866-875.
39. Downey, G.P.; Doherty, D.E.; Schwab 3rd, B.; Elson, E.L.; Henson, P.M.; Worthen, G.S. Retention of leukocytes in capillaries: Role of cell size and deformability. *J. Appl. Physiol.* **1990**, *69*, 1767-1778.
40. Sethu, P.; Sin, A.; Toner, M. Microfluidic diffusive filter for apheresis (leukapheresis). *Lab Chip* **2006**, *6*, 83-89.
41. Bruil, A.; Van Aken, W.G.; Beugeling, T.; Feijen, J.; Steneker, I.; Huisman, J.G.; Prins, H.K. Asymmetric membrane filters for the removal of leukocytes from blood. *J. Biomed. Mater. Res.* **1991**, *25*, 1459-1480.
42. Kraus, M.; Yonath, J. Leukocyte Removal Method Using A Nitrocellulose Membrane Filter Unit. US Patent 5707526, 1998.
43. Panaro, N.J.; Lou, X.J.; Fortina, P.; Kricka, L.J.; Wilding, P. Micropillar array chip for integrated white blood cell isolation and PCR. *Biomol. Eng.* **2005**, *21*, 157-162.

44. Ji, H.M.; Samper, V.; Chen, Y.; Heng, C.K.; Lim, T.M.; Yobas, L. Silicon-based microfilters for whole blood cell separation. *Biomed. Microdevices* **2008**, *10*, 251-257.
45. VanDelinder, V.; Groisman, A. Perfusion in microfluidic cross-flow: Separation of white blood cells from whole blood and exchange of medium in a continuous flow. *Anal. Chem.* **2007**, *79*, 2023-2030.
46. Huang, L.R.; Cox, E.C.; Austin, R.H.; Sturm, J.C. Continuous particle separation through deterministic lateral displacement. *Science* **2004**, *304*, 987-990.
47. Davis, J.A.; Inglis, D.W.; Morton, K.J.; Lawrence, D.A.; Huang, L.R.; Chou, S.Y.; Sturm, J.C.; Austin, R.H. Deterministic hydrodynamics: Taking blood apart. *Proc. Natl. Acad. Sci. USA* **2006**, *103*, 14779-14784.
48. Yamada, M.; Seki, M. Hydrodynamic filtration for on-chip particle concentration and classification utilizing microfluidics. *Lab Chip* **2005**, *5*, 1233-1239.
49. Zheng, S.; Liu, J.Q.; Tai, Y.C. Streamline-based microfluidic devices for erythrocytes and leukocytes separation. *J. Microelectromech. Syst.* **2008**, *17*, 1029-1038.
50. Choi, S.; Song, S.; Choi, C.; Park, J.K. Continuous blood cell separation by hydrophoretic filtration. *Lab Chip* **2007**, *7*, 1532-1538.
51. Shevkoplyas, S.S.; Yoshida, T.; Munn, L.L.; Bitensky, M.W. Biomimetic autoseparation of leukocytes from whole blood in a microfluidic device. *Anal. Chem.* **2005**, *77*, 933-937.
52. Jain, A.; Munn, L.L. Determinants of leukocyte margination in rectangular microchannels. *PLoS One* **2009**, *4*, e7104.
53. Chang, W.C.; Lee, L.P.; Liepmann, D. Biomimetic technique for adhesion-based collection and separation of cells in a microfluidic channel. *Lab Chip* **2005**, *5*, 64-73.
54. Goldsmith, H.L.; Spain, S. Margination of leukocytes in blood flow through small tubes. *Microvasc. Res.* **1984**, *27*, 204-222.
55. SooHoo, J.R.; Walker, G.M. Microfluidic aqueous two phase system for leukocyte concentration from whole blood. *Biomed. Microdevices* **2009**, *11*, 323-329.
56. Sethu, P.; Moldawer, L.L.; Mindrinos, M.N.; Scumpia, P.O.; Tannahill, C.L.; Wilhelmy, J.; Efron, P.A.; Brownstein, B.H.; Tompkins, R.G.; Toner, M. Microfluidic isolation of leukocytes from whole blood for phenotype and gene expression analysis. *Anal. Chem.* **2006**, *78*, 5453-5461.
57. Han, K.H.; Frazier, A.B. Lateral-driven continuous dielectrophoretic microseparators for blood cells suspended in a highly conductive medium. *Lab Chip* **2008**, *8*, 1079-1086.
58. Inglis, D.W.; Riehn, R.; Austin, R.H.; Sturm, J.C. Continuous microfluidic immunomagnetic cell separation. *Appl. Phys. Lett.* **2004**, *85*, 5093-5095.
59. Inglis, D.W.; Riehn, R.; Sturm, J.C.; Austin, R.H. Microfluidic high gradient magnetic cell separation. *J. Appl. Phys.* **2006**, *99*, 08K101.
60. Qu, B.-Y.; Wu, Z.-Y.; Fang, F.; Bai, Z.-M.; Yang, D.-Z.; Xu, S.-K. A glass microfluidic chip for continuous blood cell sorting by a magnetic gradient without labeling. *Anal. BioAnal. Chem.* **2008**, *392*, 1317-1324.
61. Han, K.H.; Frazier, A.B. Paramagnetic capture mode magnetophoretic microseparator for high efficiency blood cell separations. *Lab Chip* **2006**, *6*, 265-273.



62. Basabe-Desmonts, L.; Ramstrom, S.; Meade, G.; O'Neill, S.; Riaz, A.; Lee, L.P.; Ricco, A.J.; Kenny, D. Single-step separation of platelets from whole blood coupled with digital quantification by interfacial platelet cytometry (iPC). *Langmuir* **2010**, *26*, 14700-14706.
63. Triulzi, D.J.; Griffith, B.P. Blood usage in lung transplantation. *Transfusion* **1998**, *38*, 12-15.
64. Perrotta, P.L.; Synder, E.L. Platelet storage and transfusion. In *Platelets*; Michelson, A.D., Ed.; Science: Amsterdam, the Netherlands, 2007; pp. 1265-1295.
65. Brass, L.F.; Stalker, T.J.; Zhu, L.; Woulfe, D.S. Signal transduction during platelet plug formation. In *Platelets*; Michelson, A.D., Ed.; Burlington: Academic Press, 2007; pp. 319-346.
66. Petersson, F.; Aberg, L.; Sward-Nilsson, A.M.; Laurell, T. Free flow acoustophoresis: Microfluidic-based mode of particle and cell separation. *Anal. Chem.* **2007**, *79*, 5117-5123.
67. Pommer, M.S.; Zhang, Y.T.; Keerthi, N.; Chen, D.; Thomson, J.A.; Meinhart, C.D.; Soh, H.T. Dielectrophoretic separation of platelets from diluted whole blood in microfluidic channels. *Electrophoresis* **2008**, *29*, 1213-1218.
68. Dharmasiri, U.; Witek, M.A.; Adams, A.A.; Soper, S.A. Microsystems for the capture of low-abundance cells. *Annu. Rev. Anal. Chem.* **2010**, *3*, 409-431.
69. Lundahl, J.; Hallden, G.; Hallgren, M.; Skold, C.M.; Hed, J. Altered expression of CD11b/CD18 and CD62L on human monocytes after cell preparation procedures. *J. Immunol. Methods* **1995**, *180*, 93-100.
70. Fukuda, S.; Schmid-Schonbein, G.W. Centrifugation attenuates the fluid shear response of circulating leukocytes. *J. Leukocyte Biol.* **2002**, *72*, 133-139.
71. Gascoyne, P.; Mahidol, C.; Ruchirawat, M.; Satayavivad, J.; Watcharasit, P.; Becker, F.F. Microsample preparation by dielectrophoresis: Isolation of malaria. *Lab Chip* **2002**, *2*, 70-75.
72. Zimmerman, P.A.; Thomson, J.M.; Fujioka, H.; Collins, W.E.; Zborowski, M. Diagnosis of malaria by magnetic deposition microscopy. *Am. J. Trop. Med. Hyg.* **2006**, *74*, 568-572.
73. Hou, H.W.; Bhagat, A.A.S.; Chong, A.G.L.; Mao, P.; Tan, K.S.W.; Han, J.Y.; Lim, C.T. Deformability based cell margination—A simple microfluidic design for malaria-infected erythrocyte separation. *Lab Chip* **2010**, *10*, 2605-2613.
74. Bow, H.; Pivkin, I.V.; Diez-Silva, M.; Goldfless, S.J.; Dao, M.; Niles, J.C.; Suresh, S.; Han, J. A microfabricated deformability-based flow cytometer with application to malaria. *Lab Chip* **2011**, *11*, 1065-1073.
75. Mavrou, A.; Kouvidi, E.; Antsaklis, A.; Souka, A.; Tzeli, S.K.; Kolialexi, A. Identification of nucleated red blood cells in maternal circulation: A second step in screening for fetal aneuploidies and pregnancy complications. *Prenatal Diagn.* **2007**, *27*, 150-153.
76. Bianchi, D.W.; Simpson, J.L.; Jackson, L.G.; Elias, S.; Holzgreve, W.; Evans, M.I.; Dukes, K.A.; Sullivan, L.M.; Klinger, K.W.; Bischoff, F.Z.; *et al.* Fetal gender and aneuploidy detection using fetal cells in maternal blood: Analysis of NIFTY I data. *Prenatal Diagn.* **2002**, *22*, 609-615.
77. Mohamed, H.; Turner, J.N.; Caggana, M. Biochip for separating fetal cells from maternal circulation. *J. Chromatogr. A* **2007**, *1162*, 187-192.
78. Lee, D.; Sukumar, P.; Mahyuddin, A.; Choolani, M.; Xu, G. Separation of model mixtures of epsilon-globin positive fetal nucleated red blood cells and anucleate erythrocytes using a microfluidic device. *J. Chromatogr. A* **2010**, *1217*, 1862-1866.

79. Huang, R.; Barber, T.A.; Schmidt, M.A.; Tompkins, R.G.; Toner, M.; Bianchi, D.W.; Kapur, R.; Flejter, W.L. A microfluidics approach for the isolation of nucleated red blood cells (NRBCs) from the peripheral blood of pregnant women. *Prenatal Diagn.* **2008**, *28*, 892-899.
80. Wittekind, C.; Neid, M. Cancer invasion and metastasis. *Oncology* **2005**, *69*, 14-16.
81. Budd, G.T.; Cristofanilli, M.; Ellis, M.J.; Stopeck, A.; Borden, E.; Miller, M.C.; Matera, J.; Repollet, M.; Doyle, G.V.; Terstappen, L.; *et al.* Circulating tumor cells *versus* imaging-predicting overall survival in metastatic breast cancer. *Clin. Cancer Res.* **2006**, *12*, 6403-6409.
82. Cristofanilli, M.; Budd, G.T.; Ellis, M.J.; Stopeck, A.; Matera, J.; Miller, M.C.; Reuben, J.M.; Doyle, G.V.; Allard, W.J.; Terstappen, L. Circulating tumor cells, disease progression, and survival in metastatic breast cancer. *N. Engl. J. Med.* **2004**, *351*, 781-791.
83. Kaiser, J. Cancer's circulation problem. *Science* **2010**, *327*, 1072-1074.
84. Hayes, D.F.; Cristofanilli, M.; Budd, G.T.; Ellis, M.J.; Stopeck, A.; Miller, M.C.; Matera, J.; Allard, W.J.; Doyle, G.V.; Terstappen, L. Circulating tumor cells at each follow-up time point during therapy of metastatic breast cancer patients predict progression-free and overall survival. *Clin. Cancer Res.* **2006**, *12*, 4218-4224.
85. Vona, G.; Sabile, A.; Louha, M.; Sitruk, V.; Romana, S.; Schutze, K.; Capron, F.; Franco, D.; Pazzagli, M.; Vekemans, M.; *et al.* Isolation by size of epithelial tumor cells—A new method for the immunomorphological and molecular characterization of circulating tumor cells. *Am. J. Pathol.* **2000**, *156*, 57-63.
86. Zabaglo, L.; Ormerod, M.G.; Parton, M.; Ring, A.; Smith, I.E.; Dowsett, M. Cell filtration-laser scanning cytometry for the characterisation of circulating breast cancer cells. *Cytometry, Part A* **2003**, *55A*, 102-108.
87. Mohamed, H.; Murray, M.; Turner, J.N.; Caggana, M. Isolation of tumor cells using size and deformation. *J. Chromatogr. A* **2009**, *1216*, 8289-8295.
88. Zheng, S.; Lin, H.; Liu, J.-Q.; Balic, M.; Datar, R.; Cote, R.J.; Tai, Y.-C. Membrane microfilter device for selective capture, electrolysis and genomic analysis of human circulating tumor cells. *J. Chromatogr. A* **2007**, *1162*, 154-161.
89. Hosokawa, M.; Hayata, T.; Fukuda, Y.; Arakaki, A.; Yoshino, T.; Tanaka, T.; Matsunaga, T. Size-selective microcavity array for rapid and efficient detection of circulating tumor cells. *Anal. Chem.* **2010**, *82*, 6629-6635.
90. Tan, S.J.; Yobas, L.; Lee, G.; Ong, C.; Lim, C.T. Microdevice for the isolation and enumeration of cancer cells from blood. *Biomed. Microdevices* **2009**, *11*, 883-892.
91. Saias, L.; Saliba, A.E.; Viovy, J.L.; Pierga, J.Y.; Vielh, P.; Farace, F. Microfluidic magnetic cell sorting system for cancer diagnosis. *Houille Blanche* **2009**, *5*, 105-111.
92. Gleghorn, J.P.; Pratt, E.D.; Denning, D.; Liu, H.; Bander, N.H.; Tagawa, S.T.; Nanus, D.M.; Giannakakou, P.A.; Kirby, B.J. Capture of circulating tumor cells from whole blood of prostate cancer patients using geometrically enhanced differential immunocapture (GEDI) and a prostate-specific antibody. *Lab Chip* **2010**, *10*, 27-29.
93. Nagrath, S.; Sequist, L.V.; Maheswaran, S.; Bell, D.W.; Irimia, D.; Ulkus, L.; Smith, M.R.; Kwak, E.L.; Digumarthy, S.; Muzikansky, A.; *et al.* Isolation of rare circulating tumour cells in cancer patients by microchip technology. *Nature* **2007**, *450*, 1235-1239.

94. Adams, A.A.; Okagbare, P.I.; Feng, J.; Hupert, M.L.; Patterson, D.; Gottert, J.; McCarley, R.L.; Nikitopoulos, D.; Murphy, M.C.; Soper, S.A. Highly efficient circulating tumor cell isolation from whole blood and label-free enumeration using polymer-based microfluidics with an integrated conductivity sensor. *J. Am. Chem. Soc.* **2008**, *130*, 8633-8641.
95. Spizzo, G.; Gastl, G.; Obrist, P.; Went, P.; Dirnhofer, S.; Bischoff, S.; Mirlacher, M.; Sauter, G.; Simon, R.; Stopatschinskaya, S.; *et al.* High Ep-CAM expression is associated with poor prognosis in node-positive breast cancer. *Breast Cancer Res. Treat.* **2004**, *86*, 207-213.
96. Lee, J.M.; Dedhar, S.; Kalluri, R.; Thompson, E.W. The epithelial-mesenchymal transition: New insights in signaling, development, and disease. *J. Cell Biol.* **2006**, *172*, 973-981.
97. Thompson, E.W.; Newgreen, D.F.; Tarin, D. Carcinoma invasion and metastasis: A role for epithelial-mesenchymal transition? *Cancer Res.* **2005**, *65*, 5991-5995.
98. Dharmasiri, U.; Balamurugan, S.; Adams, A.A.; Okagbare, P.I.; Obubuafo, A.; Soper, S.A. Highly efficient capture and enumeration of low abundance prostate cancer cells using prostate-specific membrane antigen aptamers immobilized to a polymeric microfluidic device. *Electrophoresis* **2009**, *30*, 3289-3300.
99. Xu, Y.; Phillips, J.A.; Yan, J.L.; Li, Q.G.; Fan, Z.H.; Tan, W.H. Aptamer-based microfluidic device for enrichment, sorting, and detection of multiple cancer cells. *Anal. Chem.* **2009**, *81*, 7436-7442.
100. Cohen, J. The immunopathogenesis of sepsis. *Nature* **2002**, *420*, 885-891.
101. Edmond, K.; Zaidi, A. New approaches to preventing, diagnosing, and treating neonatal sepsis. *PLoS Med.* **2010**, *7*, e1000213.
102. Wu, Z.G.; Willing, B.; Bjerketorp, J.; Jansson, J.K.; Hjort, K. Soft inertial microfluidics for high throughput separation of bacteria from human blood cells. *Lab Chip* **2009**, *9*, 1193-1199.
103. Mach, A.J.; Di Carlo, D. Continuous scalable blood filtration device using inertial microfluidics. *Biotechnol. Bioeng.* **2010**, *107*, 302-311.
104. Xia, N.; Hunt, T.; Mayers, B.; Alsberg, E.; Whitesides, G.; Westervelt, R.; Ingber, D. Combined microfluidic-micromagnetic separation of living cells in continuous flow. *Biomedical Microdevices* **2006**, *8*, 299-308.
105. Yung, C.W.; Fiering, J.; Mueller, A.J.; Ingber, D.E. Micromagnetic-microfluidic blood cleansing device. *Lab Chip* **2009**, *9*, 1171-1177.